



Synthesis, characterization and spectral estimation of Nickel (II) and Copper (II) complexes and study of their antibacterial activity

Muhammed N. Tawfeeq^{1,*}, Eman Thiab Al Samarrai², Sattar R. Majeed³

¹Iraqi Ministry of Education - Anbar Education, Ramadi, Anbar, Iraq

²Department of Chemistry, College of Education, Univ. Of Samarra, Iraq

³Department of Chemistry, College of Science, Univ. Of Anbar, Ramadi, Anbar, Iraq

ARTICLE INFO

Article history:

Received 24 August 2024

Received in revised form 3 November 2024

Accepted 6 November 2024

Available online 4 December 2023

Keywords:

Azo ligand

Nickel(II) Complexes

Copper(II) Complexes

Spectroscopic methods

ABSTRACT

The study includes the synthesis and characterization of new azo compound 4-((2-amino-5-nitrophenyl)diazenyl)benzenesulfonic acid (ANBS) as reagent and their complexes with the two metals nickel (II) and copper (II). The complexes were prepared by mixing the azo ligand as a primary ligand and sodium pyrophosphate (pyph) and malonic acid (ma) as secondary ligands using metal-ligand in a 1:1:1 mole ratio. Reagent and complexes were characterized by spectroscopic methods FTIR, UV-Visible, Atomic absorption, C.H.N and GC-Mass. The in-vitro biological activity of the ligand and the metal complexes were screened against the Gram-negative and Gram-positive pathogenic bacteria *Serratia marcescens* and *Pseudomonas aeruginosa*. The copper complexes showed high efficiency of antimicrobial activity compared with the ligand. Spectroscopic methods were developed to estimate nickel and copper, the best conditions was study which gave high sensitivity. It showed Linear range at 1-10 ppm with a correlation coefficient of (0.9901-0.9924). The detection limit was between (0.0715-0.0895) and the quantitative limit was between (0.2166-0.2713) ppm, the Sandel sensitivity was between (0.0166-0.0208) $\mu\text{g}/\text{cm}^2$ and the Recovery% was (100.6177-101.4508).

1. Introduction

This study focuses on the synthesis, biological, and analytical properties of azo ligands with metal complexes [1], which have significant importance in chemical analysis due to the toxicity of the elements, especially nickel, copper and others, and their serious effects on the ecosystem in general and on humans and animals in particular [2]. Finding quick methods to process it and determine concentrations, on the other hand, the importance of metal complexes lies in their wide biological activity, such as anti-cancer [3,4], anti-bacterial [5], and anti-fungal [6]. Studies indicate that azo complexes have better effectiveness compared to azo ligands [7], which increase their effectiveness by increasing the azo bonds within the compound, which

leads to the accumulation of antibacterial activity [8]. Complexes prepared from azo bonds of acetophenone precursors showed good inhibitory activity against a variety of bacteria and cancer cells [9]. These ligands have applications in industrial and pharmaceutical industries [10], including textile dyeing, antimicrobial, antifungal, anti-inflammatory, antihypertensive, and antiviral drugs [11]. Diazonium salts are synthetic intermediates that undergo coupling reactions to form azo dyes organic compounds with aryl functional groups $\text{R}-\text{N}=\text{N}$. These dyes are used as primary building blocks in organic compounds with emerging commercial and biological properties. Temperature, acidic concentration and sodium nitrite pH play crucial roles in diazotization. Azo dyes have a backbone Auxochrome, chromophoric, and solubilizing groups and their color is determined by azo bonds [12].

* Corresponding author; mohamed_tawfiq@uosamarra.edu.iq

<https://doi.org/10.22034/crl.2024.474953.1411>



This work is licensed under Creative Commons license CC-BY 4.0

Azo dyes are non-biodegradable and harmful to the environment, as they accumulate in oceans and affect marine life. Direct dyes are carcinogenic and have negative reproductive effects, while reactive dyes are linked to increased allergy risk. Although many countries have banned azo dyes they are still present in the market, with approximately 2000 currently in use. Some azo dyes are known for their toxic and genotoxic properties, and their use in laboratories is a concern due to their environmental impact. Azo dyes are a diverse group of synthetic dyes used in various industries, including pharmaceuticals, cosmetics, paper, plastics, and food colors. They are commonly used in inkjet printing, thermal transfer printing, photography, biomedical areas, molecular recognition, light-controlled polymers, and the liquid crystal industry [13].

The azo dye reaction is considered an electrophilic aromatic substitution reaction [14], as the diazonium salts behave electrophilically and carry a positive charge. As for the conjugated ring, it represents a nucleophile, where the positive part is attacked, and the compensation site is according to the compensating group on the conjugated ring. The driving groups on the ring give compensation at the ortho and para sites, and the para site is preferred because the resonance states of the ring increase, while the groups pulling on the ring give compensation at the meta site [15,16].

Recently, several methods have been found to prepare azo compounds, including direct oxidation of aromatic amines using catalysts, where transition elements such as copper were used due to their ability to change their oxidative state, and then developed using nanoparticles, which gave high productivity and selectivity [17,18]. Azo compounds were also prepared from the reduction of nitro-aromatic compounds. Using palladium and gold nanoparticles as catalysts for the reduction of the nitro group and the formation of azo compounds [19,20].

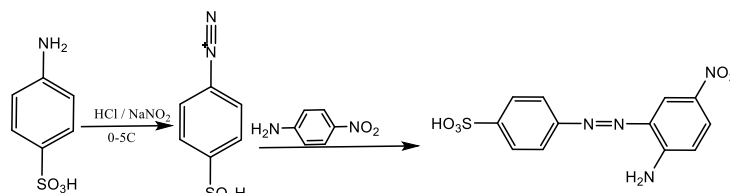
2. Materials and Methods

All experiments were used materials high pure chemical. Nickel(II) chloride hydrate $\text{NiCl}_2 \cdot 6\text{H}_2\text{O}$ (BDH 99%), Copper(II) chloride hydrate $\text{CuCl}_2 \cdot 2\text{H}_2\text{O}$ (BDH 99%), Oxalic-acid (Fluka 99.5%), Malonic acid, (Fluka 99.5%) tetra Sodium pyrophosphate (Fluka 99%), 4-amino sulfonic acid (Aldrich 98%), 4-nitro aniline (Fluka 98%), DMSO (HiMedia 99%) and ethanol (Honeywell 99.8%). Shimadzu Atomic Absorption/Flame Emission Spectrophotometer (AA680), electro thermal melting point, C.H.N Vectro model EA3000 single, Infrared spectra were determined (Shimadzu (FT-IR)-8400S, Japan), single-beam (U.V-Vis) spectrophotometer (U.V (N4S) China), The chlorine content of the prepared

complexes was measured using Moore's method 686-titro processor-665 and mass spectra by GC-mass QP SO A: shima 170 ev).

2.1 Synthesis of Azo ligand (ANBS) ($\text{C}_{12}\text{H}_{10}\text{N}_4\text{O}_5\text{S}$)

After dissolving 4-amino benzene sulfonic acid (0.433g, 2.5 mmol) in 30 ml of water over a few minutes after cooling the solution and add 2.0 ml of hydrochloric acid while stirring, a clear solution was produced. A $0^\circ\text{--}5^\circ\text{C}$ temperature range was maintained. Next, an aqueous solution containing 1g of sodium nitrite that is dissolved in 10ml of water has been gradually added, dropwise, while maintaining the temperature below 5°C . The mixture was after that stirred for five minutes. An ice bath was used to cool the 0.345g, 2.5 mmol 4-nitro aniline after it had been dissolved in 10 ml of ethanol. The final solution (solution 1) was combined with cooling. Following drying, the precipitate produced was filtered, and as shown in Scheme 1, The ligand was repurified by adding methanol as a partially dissolving solvent, and the solution was filtered and left to dry. a dark red solid precipitate with a yield of 76.9% and a melting point of 190°C was obtained [21].



Scheme 1: Synthesis azo ligand (ANBS)

2.2 Synthesis of complexes:

2.2.1 preparation of $[\text{Ni}(\text{ANBS})\text{Cl}_2]$ complex:

0.5 mmol (0.161g) of (ANBS) ligand diluted in 20 mL ethanol were combined with 0.5 mmol (0.065g) of $\text{NiCl}_2 \cdot 6\text{H}_2\text{O}$. After combining the two solutions, the pH was raised to 6 and the mix refluxed for 3hrs at 50°C . After cooling and filtering the solution, it was repeatedly cleaned with ethanol and after that dried diethyl ether [22], a reddish a grey solid precipitate with a yield of 68.8% and a melting point of more than 300°C was obtained.

2.2.2 preparation of $[\text{Cu}(\text{ANBS})\text{Cl}_2]$ complex:

0.5 mmol (0.161g) of (ANBS) ligand diluted in 20 mL ethanol were combined with 0.5 mmol (0.085g) of $\text{CuCl}_2 \cdot 2\text{H}_2\text{O}$. After combining the two solutions, the pH was raised to 6 and the mix refluxed for 3hrs at 50°C . After cooling and filtering the solution, it was repeatedly

cleaned with ethanol and after that dried diethyl ether [22], a grey solid precipitate with a yield of 74.1% and a melting point of more than 300 °C was obtained.

2.2.3 preparation of [Ni(ANBS) (pyph)] and [Cu(ANBS)(H₂O)₂(ma)]

The mixed complexes have been prepared in molar ratios of 1:1:1, where the previous preparation was repeated and secondary ligands were added to it (tetra-sodium pyrophosphate 0.5 mmol (0.223g) (yield 74.6%) and malonic acid 0.5 mmol (0.052g) (yield 77.4%) [22].

2.3 Reagent and chemical solutions

The reagent solution (1000 µg/ml) was prepared by dissolving 0.1 g of ligand in a small amount of ethanol, transferred to 100 ml volumetric flask and supplemented to the mark with the same solvent. Nickel(II) ion solution (1000 µg/ml) prepare by taking 0.4 g of NiCl₂.6H₂O in an amount of distilled water, then transfer it to a 100 ml volumetric flask and fill to the mark with distilled water. Copper(II) ion solution (1000 µg/ml) prepare by taking 0.268 g of CuCl₂.2H₂O in an amount of distilled water, then transfer it to a 100 ml volumetric vial and fill to the mark with distilled water. Hydrochloric acid solution (0.1 M) prepare by diluting 0.83 ml of concentrated acid to 11.97 molarity by adding it to distilled water and bringing the volume to the mark in a 100 ml bottle. Sodium hydroxide solution (0.1M) prepare by dissolving 0.4 g of sodium hydroxide in an amount of distilled water, transferred it to a 100 ml volumetric vial and completing the volume with distilled water. Buffer solution (pH=6.0) dissolve 1.36 g of KH₂PO₄ in distilled water and transfer it to a 100 ml bottle. Complete the volume with distilled water to become 0.1 molar, then withdraw 50 ml of it and put it in a 100 ml bottle and add 5.6 ml of NaOH, concentration 0.1 M, then complete the volume with distilled water. Buffer solution (pH = 12.7) dissolve 1.49 grams of KCl in a 100 ml bottle and complete the volume until its concentration is 0.2 M. 25 ml of it was withdrawn and placed in a 100 ml bottle. 32.2 ml of NaOH, 0.1 M concentration, was added to the bottle, then the volume was completed with distilled water [23]. Solutions of the compounds were prepared at a concentration (1000 µg/ml) where 0.1 g was dissolved in DMSO solvent, and the volume was completed in a 100-ml volumetric flask.

2.4 Preparing the culture medium for bacteria

Muller Hinton agar (MHA) culture medium was prepared by dissolving 38 g of agar in 1 liter of distilled water in a conical flask, heating and stirring with a magnetic stirrer until dissolution was complete, and then transferring it to

an autoclave at 121 °C. °C and at a pressure of 1.5. In the air for half an hour, the solution was cooled, then 20 ml of the medium was poured into several sterile Petri dishes and left to solidify [24]. The effectiveness of the prepared compounds was tested on bacteria samples in the laboratories of the Department of Biotechnology / College of Science / Anbar University, where a volume of 70 microliters was injected into each hole for each prepared material and at several concentrations from 100-1000 ppm.

3. Results

3.1 Elemental microanalysis and some physical characteristics

Elemental microanalysis (C.H.N) with metal and some of the physical characteristics have been listed in Table 1.

Table 1: Elemental microanalysis and some physical characteristics

Compound	C%	H%	N%	M%	Cl%	Melting point
(ANBS) (C ₁₄ H ₁₂ N ₂ O ₅ S)	44.68 (44.10)	3.10 (4.08)	17.37 (18.41)	-----	-----	190
[Ni (ANBS)Cl ₂]	32.01 (32.11)	2.22 (1.59)	12.45 (13.42)	13.05 (13.59)	15.78 (16.37)	300<
[Cu (ANBS)(H ₂ O) ₂ Cl ₂]	29.33 (28.74)	2.85 (1.98)	11.40 (10.87)	12.93 (12.64)	14.25 (15.19)	300<

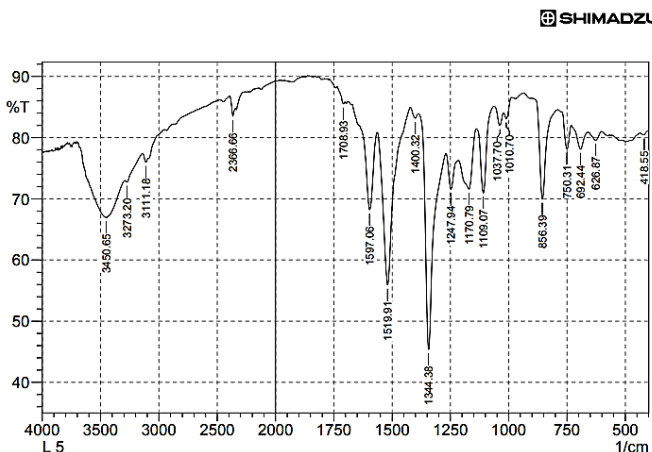


Fig 1a: IR spectrum of (ANBS) (C₁₂H₁₀N₄O₅S)

3.2 FT-IR spectral data

The infrared spectra of the ligand and their complexes are summarized in Table 2, Fig 1a-e where the amine group bands (3450)cm⁻¹, (3273)cm⁻¹ to NH₂[25] asymmetrical and symmetrical respectively showed a shift towards lower frequencies in the complexes, There was also a slight change in the frequencies of the azo group bands, which appeared in the range (1400-1460) cm⁻¹[26], which indicates the occurrence of coordination and the appearance of new bands belonging to the secondary

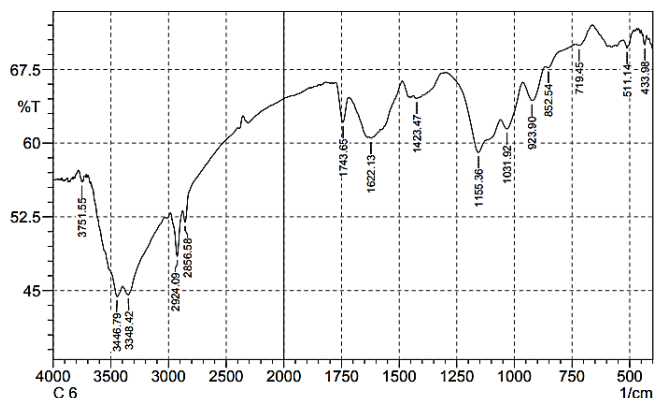
bonds at 1363 and 1278 cm^{-1} for the complex $[\text{Cu}(\text{ANBS})(\text{H}_2\text{O})_2(\text{ma})]$ which is due to the asymmetric and symmetrical stretching of $-\text{COO}$ group, and bands appeared in the range (1577-1633) cm^{-1} that belong to the $\text{C}=\text{C}$ group. There are also weak bands in the range 400 cm^{-1} and 500 cm^{-1} , which are resulting from the bonding of donor atoms to the metal (M-N) and (M-O) [27].

SHIMADZU

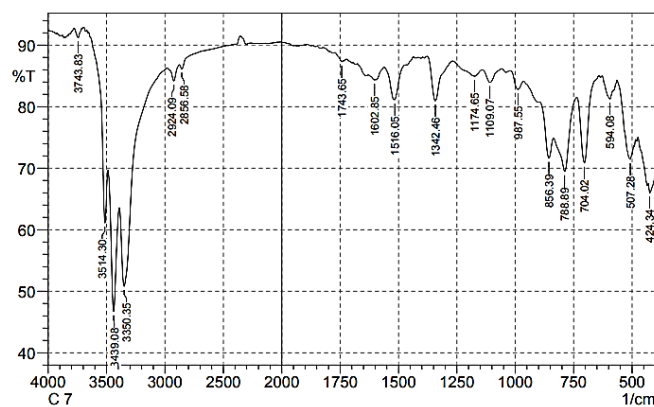
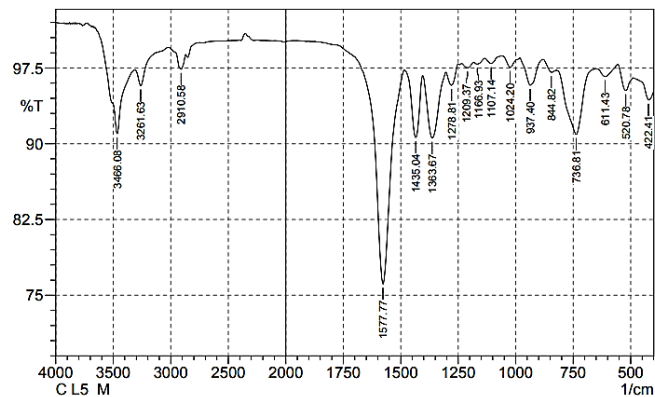
Table 2: IR data for ligand and their complexes

Compounds	NH ₂ U _{as} y	NH ₂ U _{sy}	N= N	CO O U _{as} y	CO O U _{sy}	P= O	M- N	M- O
(ANBS)(C ₁₂ H ₁₀ N ₄ O ₅ S)	345 0	327 3	140 0	----- -	----- -	----- -	----- -	----- -
[Ni (ANBS) Cl ₂]	344 6	334 8	142 3	----- -	----- -	----- -	43 3	51 1
[Cu (ANBS)(H ₂ O) ₂ Cl ₂]	343 9	335 0	146 0	----- -	----- -	----- -	42 4	50 7
[Ni(ANBS)(pyph)]	342 7	322 0	152 1	----- -	----- -	910	49 3	57 0
[Cu(ANBS)(H ₂ O) ₂ (m a)]	346 6	326 1	143 5	136 3	127 8	----- -	42 2	52 0

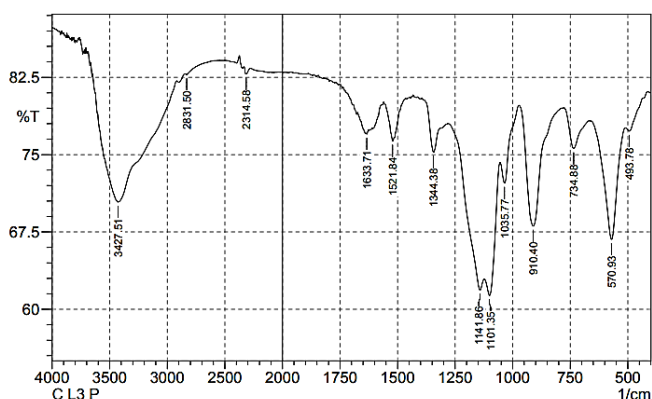
SHIMADZU

**Fig 1b:** IR spectrum of $[\text{Ni}(\text{ANBS})\text{Cl}_2]$

SHIMADZU

**Fig 1c:** IR spectrum of $[\text{Cu}(\text{ANBS})(\text{H}_2\text{O})_2\text{Cl}_2]$ **Fig 1d:** IR spectrum of $[\text{Cu}(\text{ANBS})(\text{H}_2\text{O})_2(\text{ma})]$

SHIMADZU

**Fig 1e:** IR spectrum of $[\text{Ni}(\text{ANBS})(\text{pyph})]$

3.3 U.V-Vis Spectral data

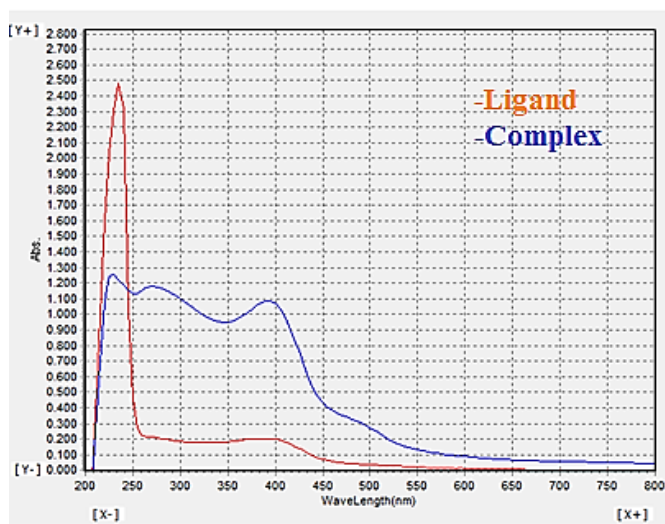
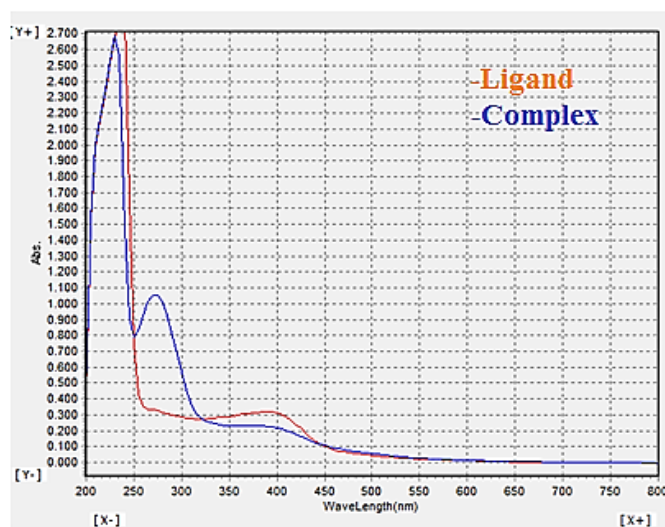
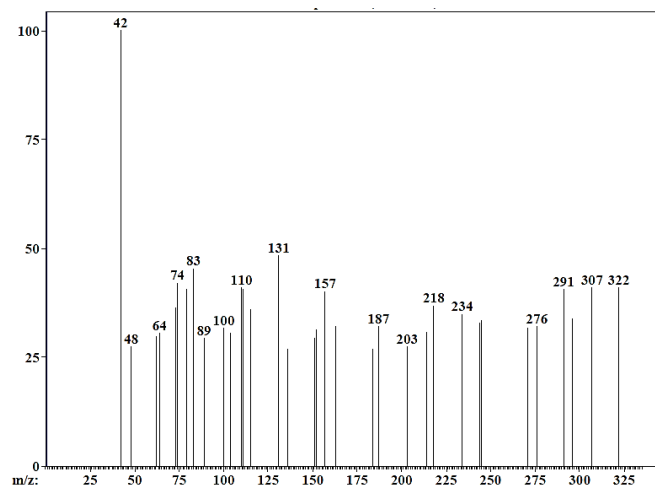
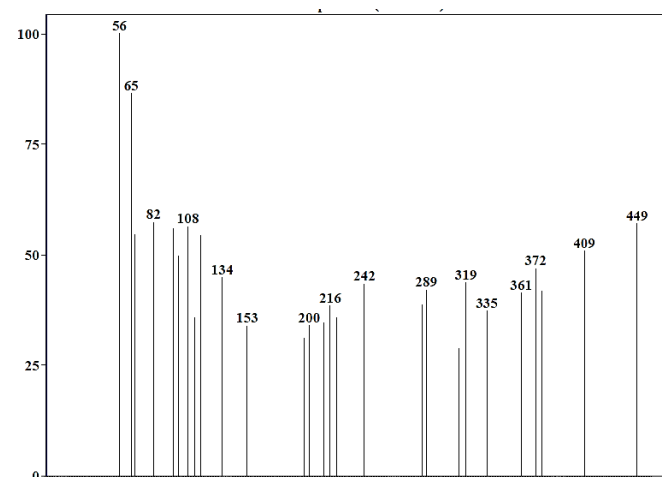
Table 3 and Figs. 2a-d provides an overview of the UV spectrum data for the complex of ligand, Ni(II), and copper(II). In each case, the spectrum for the ligand showed an intense absorption peak in UV region at 240 nm and 279 nm indicating ($\pi \rightarrow \pi^*$) and at (388) nm indicates ($n \rightarrow \pi^*$). The spectra of the complexes for $[\text{Ni}(\text{ANBS})\text{Cl}_2]$ complex showed the appearance of a new absorption peak at (485) nm and (400) nm for $[\text{Cu}(\text{ANBS})(\text{H}_2\text{O})_2\text{Cl}_2]$ complex, , while in the mix ligand complex $[\text{Cu}(\text{ANBS})(\text{H}_2\text{O})_2(\text{ma})]$ a peak appeared at 586 nm to the transition ($d-d$) ${}^2T_{1g} \rightarrow {}^2E_g$ and 597 nm for $[\text{Ni}(\text{ANBS})(\text{pyph})]$ complex to the transition ($d-d$) ${}^3A_{2g} \rightarrow {}^3T_{1g}$ [28,29].

3.4 Mass spectra of ligands and complexes

Figure 3a displays mass spectrum of the ligand (ANBS). The mass spectrum of ligand with a molecular weight of (323), which produced a parent peak at $m/z = 322$ (M^+). Figure 3b displays the complex $[\text{Ni}(\text{ANBS})\text{Cl}_2]$ mass spectrum, which revealed a parent peak at $m/z = 449$ (M^+).

Table 3: UV spectrum data for ligand and complex

No	Compounds	λ_{\max} nm	Transition Assignment
1	(ANBS) ($C_{12}H_{10}N_4O_5S$)	240	$^*\pi \rightarrow \pi$
		279	$^*\pi \rightarrow \pi$
		388	$n^* \rightarrow \pi$
2	$[Ni(ANBS)Cl_2]$	229	$^*\pi \rightarrow \pi$
		275	$^*\pi \rightarrow \pi$
		394	$n^* \rightarrow \pi$
		485	C.T
3	$[Cu(ANBS)(H_2O)_2Cl_2]$	230	$^*\pi \rightarrow \pi$
		274	$^*\pi \rightarrow \pi$
		400	C.T
4	$[Cu(ANBS)(H_2O)_2(ma)]$	281	$^*\pi \rightarrow \pi$
		394	$n^* \rightarrow \pi$
		586	$^2T_{1g} \rightarrow ^2E_g$
5	$[Ni(ANBS)(pyph)]$	283	$^*\pi \rightarrow \pi$
		404	C.T
		597	$^3A_{2g} \rightarrow ^3T_{1g}$

Fig 2a: Electronic spectrum of $[Ni(ANBS)Cl_2]$ Fig 2b: Electronic spectrum of $[Cu(ANBS)(H_2O)_2Cl_2]$ Fig 3a: Mass spectrum of (ANBS) ($C_{12}H_{10}N_4O_5S$)Fig 3b: Mass spectrum of complex $[Ni(ANBS)Cl_2]$

Analytical methods

Easy and fast spectroscopic methods were developed to estimate nickel(II) and copper(II) using the prepared reagents. The maximum wavelength for each complex was determined and the best conditions were studied (the effect of the solvent, the effect of acid and base, effect of buffer solution, effect of temperature and time) Table 4a-e, which helped in improving the absorption values.

Table 4a: The effect of the solvent

Compound	Water	Ethanol	Acetone
$[Ni(ANBS)Cl_2]$	0.132	0.175	0.098
$[Cu(ANBS)(H_2O)_2Cl_2]$	0.399	0.514	0.430

It appears from the table above that the best solvent was ethanol to give it the highest absorption.

Table 4b: Effect of acid and base

Compound	HCl (0.1M) VmL	A	pH	NaOH (0.1M) Vml	A	pH
[Ni(ANBS)Cl ₂]	0	0.175	7.1	0	0.175	7.1
	0.1	0.088	2.1	0.1	0.321	10.4
	0.2	0.082	1.9	0.2	0.336	11.8
	0.3	0.078	1.8	0.3	0.340	12.5
	0.4	0.075	1.8	0.4	0.344	12.7
				0.5	0.350	12.8
[Cu(ANBS) (H ₂ O) ₂ Cl ₂]	0	0.514	6.0	0	0.514	6.0
	0.1	0.508	2.0	0.1	0.414	10.0
	0.2	0.508	1.8	0.2	0.414	12.1
	0.3	0.507	1.8	0.3	0.418	12.5

We conclude from the table above that adding acid to the nickel complex reduces the absorption value, but when adding the base, the absorption values increase, so the addition of the base was fixed for subsequent experiments. As for the copper complex, adding acid or base reduces the absorption, so it was excluded in subsequent experiments.

Table 4c: Effect of buffer solution

Compound	Buffer (12.7) VmL	A (485nm)
[Ni(ANBS)Cl ₂]	0	0.344
	0.1	0.349
	0.2	0.356
	0.3	0.364
	0.4	0.449 (turbid)
[Cu(ANBS) (H ₂ O) ₂ Cl ₂]	Buffer (6.0) VmL	A (400nm)
	0	0.514
	0.1	0.521
	0.2	0.558
	0.3	0.583
	0.4	0.649 (turbid)

From the table above, the absorption increased when adding the buffer solution, so it was confirmed in subsequent experiments

Table 4d. Effect of temperature

Compound	T(c°)	A(485nm)
[Ni(ANBS)Cl ₂]	5	0.338
	10	0.341
	15	0.347
	20	0.359
	25	0.364
	30	0.367
	35	0.371
	40	0.363
	45	0.364
	50	0.362
	55	0.360
[Cu(ANBS) (H ₂ O) ₂ Cl ₂]	T(c°)	A(400nm)
	5	0.483
	10	0.491
	15	0.502
	20	0.544
	25	0.583
	30	0.625
	35	0.628
	40	0.621
	45	0.623
50	0.624	
55	0.619	

Table 5. The analytical parameters

Compound	λ_{max} nm	Linear range	Slope	Molar Absorptivity (Lmol ⁻¹ cm ⁻¹)	LOD (µg/mL)	LOQ (µg/mL)	Sandell's Sensitivity (µg/cm ²)	% Rec
[Ni(ANBS)Cl ₂]	485	5-40	0.0479	21550	0.0895	0.2713	0.0208	101450
[Cu(ANBS) (H ₂ O) ₂ Cl ₂]	400	5-40	0.06	29455	0.0715	0.2166	0.0166	100617

From the table above, increasing the temperature increases absorption, so the optimal temperature for each complex was fixed. From the above table, we conclude that the complex is stable over a wide period of time.

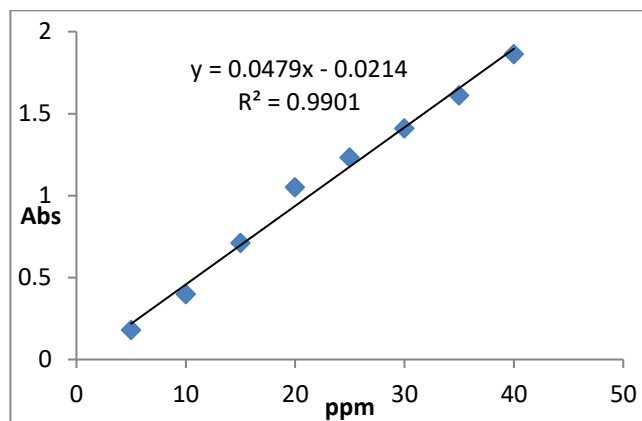
3.5 Calibration curve

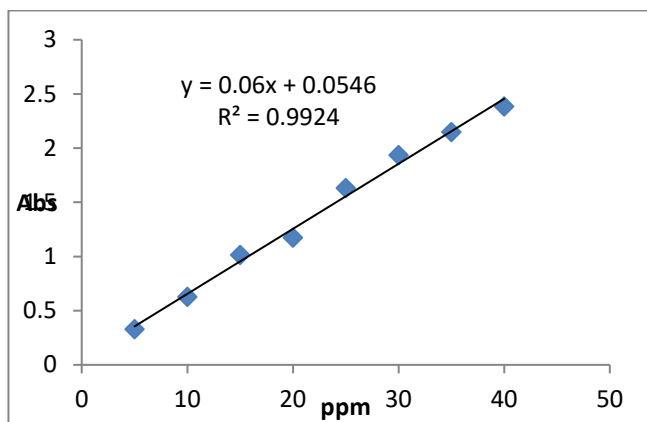
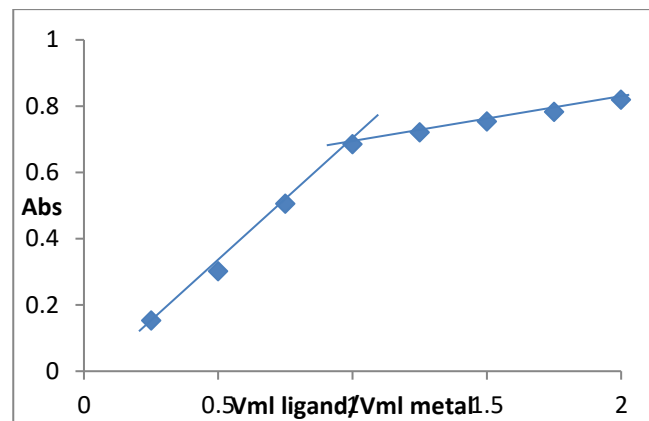
The calibration curve was prepared by taking increasing volumes of each of the metal and the reagent (0.1-1.5) ml. The previous conditions were applied to each complex, and the volumes were completed to the mark with ethanol and heated at the optimal temperature for each complex. Then the absorbance of the solutions was

Table 4e. Effect of time

Min	5	15	25	35	45	60
[Ni(ANBS)Cl ₂]	0.370	0.373	0.374	0.373	0.372	0.371
[Cu(ANBS)(H ₂ O) ₂ Cl ₂]	0.626	0.628	0.628	0.625	0.627	0.629

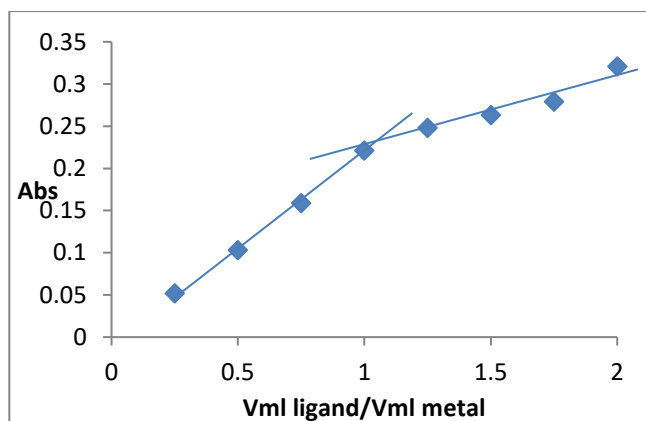
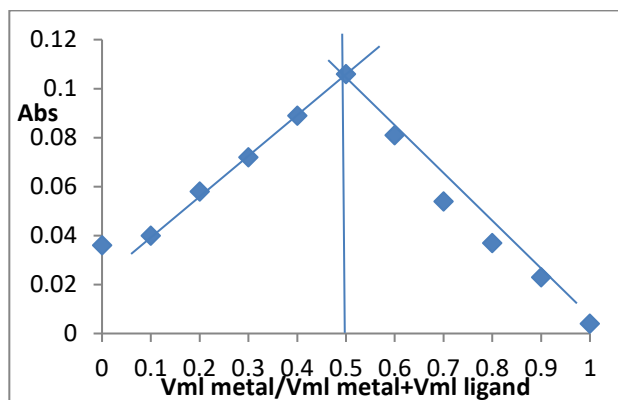
measured at the specific wavelength for each complex, as shown in Fig 4a-b, , where the linear range from (5-40) ppm, and the estimation factor ranges at (0.9901-0.9924). To express the accuracy and precision, the standard deviation, standard deviation, detection limit, quantification limit, and Sandel sensitivity were calculated, and the analytical parameters of the methods are summarized in Table 5 [30]. Table 6 shows the comparison of the proposed method with other methods.

Fig 4a. Calibration curve for the complex [Ni(ANBS)Cl₂]

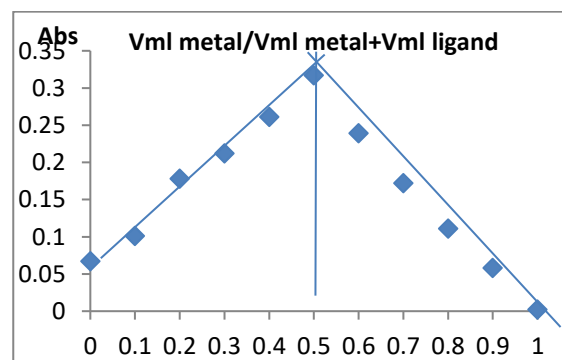
Fig 4b: Calibration curve for the complex $[Cu(ANBS) (H_2O)_2Cl_2]$ Fig 5c: Molar ratio of complex $[Cu(ANBS) (H_2O)_2Cl_2]$

3.6 Molar ratio and Job's approach of continuous variation

The ratio of ligand to metal was determined using the Job method[34,35] and the molar ratios[36] the ratio of both Ni (II) and Cu(II) with reagent has been varied and the absorbance of the resulting mixtures have been recorded at 485 nm for nickel complex and 400 nm for copper complex. This was found at 1:1 (M:L) Ni(II): (ANBS) also Cu(II): (ANBS)As shown in the Fig 5a-d.

Fig 5a: Molar ratio of complex $[Ni(ANBS)Cl_2]$ Fig 5b: job method of complex $[Ni(ANBS)Cl_2]$

Me tal	Reagent	λ_{max} nm	Linaer range	Molar Absorptivity ($Lmol^{-1}cm^{-1}$)	Refer ences
Ni	nicotinohydroxamic acid	530	2.57-6.85	1.371×10^4	[31]
	aminophenols [2-piperidinomethyl-4-(1-methylcyclopentyl) phenol	450	0.04-3.8	1.75×10^4	[32]
	2-piperidinomethyl-4-(1-methylcyclohexyl) phenol	465	0.03-4.2	2.94×10^4	
	2-piperidinomethyl-4-(3-methylcyclohexyl) phenol	475	0.04-4.0	2.53×10^4	
	(ANBS)	485	5-50	2.1550×10^4	Prop osed meth od
Cu	(ANBS)	470	0.5-5.0	6.55×10^3	[33]
	aminophenols [2-piperidinomethyl-4-(1-methylcyclopentyl) phenol	545	0.03-3.6	3.05×10^4	[32]
	2-piperidinomethyl-4-(1-methylcyclohexyl) phenol	542	0.02-3.8	4.05×10^4	
	2-piperidinomethyl-4-(3-methylcyclohexyl) phenol	533	0.04-3.6	3.25×10^4	
	(ANBS)	400	5-50	2.9455×10^4	Prop osed meth od

Fig 5d. job method of complex $[Cu(ANBS) (H_2O)_2Cl_2]$

3.7 The suggested structural formula of prepared Ni(II) and Cu(II) complexes

The geometric shapes of the prepared complexes were proposed, as square planar because of the strong field of ligand and its dsp^2 hybridization were proposed for nickel (II) complexes [37] and octahedral and Sp^3d^2 hybridization copper (II) complexes, as shown in the Table 7 [38].

3.8 Biological activities

The antibacterial activity of ligands and metal complexes, was tested on four species of bacteria namely: Pseudomonas, Klebsiella pneumoniae, Candida aureus, E. coli, Staphylococcus aureus and Serratia marcescens by measuring the diameters of inhibition zone on the Muller Hinton agar plates. The Inhibitory effects of $[Cu(ANBS)(H_2O)_2(pyph)]$ as in Table 8 and Fig 6, $[Cu(ANBS)(H_2O)_2Cl_2]$ and $[Ni(ANBS)(pyph)]$. Our observation indicated that activity. Activity 35, 24 with $[Cu(ANBS)(H_2O)_2Cl_2]$ with $[Ni(ANBS)(pyph)]$ showed best antimicrobial activity against Serratia marcescens (Gram-negative). That was confirmed by the literature [5]. This may be due to its effect on the peptidoglycan, the layer of cell wall which is thicker in Gram-positive than Gram-negative bacteria [39]. On the other hand, the $[Cu(ANBS)(H_2O)_2Cl_2]$ (1000 ppm) showed the highest antibacterial activity. This may be attributed to obtaining the highest percentage of copper metal, as this was evident from the complexes distribution. One possible way of the mechanism of action of complexes involves wrapping around the bacterial cells and trapping them. Moreover, direct contact of bacterial cells can cause damage to the plasma membrane, leading to intracellular substance leakage and adversely affecting cellular metabolism [40,41] complexes also have a relatively large surface area, which makes their complexes capable of inactivating the cells of microorganisms [42]. Cell morphology plays an important role in the bactericidal efficacy of the metal complexes. Gram-negative and Gram-positive bacteria have different chemical compositions and cell wall structures.

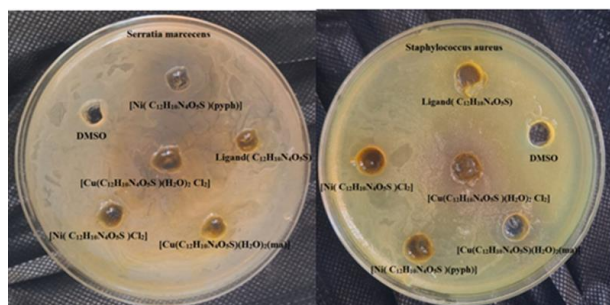


Fig. 6. Bacteriostatic activity of Serratia marcescens and Staphylococcus aureus

No	Complexes	The molecular structure
1	$[Ni(ANBS)Cl_2]$ Dichloro(4-((2-amino-5-nitrophenyl)diazanyl)benzene sulfonic acid) nickel(II)	
2	$[Cu(ANBS)(H_2O)_2Cl_2]$ Diaquadichloro(4-((2-amino-5-nitrophenyl)diazanyl)benzene sulfonic acid) copper(II)	
3	$[Ni(ANBS)(pyph)]$ pyrophosphato(4-((2-amino-5-nitrophenyl)diazanyl)benzene sulfonic acid) nickel(II)	
4	$[Cu(ANBS)(H_2O)_2(ma)]$ Diaquamalonato(4-((2-amino-5-nitrophenyl)diazanyl)benzene sulfonic acid) copper(II)	

In comparison to the thin layer of peptidoglycan in the cell wall of Gram-negative bacteria, Gram-positive bacteria have a thick cell wall consisting of several layers of peptidoglycan [43,44].

Table 8. Bacterial activity results

Compounds	DM SO	Serratia marcescens	Staphylococcus aureus	E. coli	Candida aureus	Klebsiella pneumoniae	Pseudomonas
(ANBS) $C_{12}H_{18}N_4O_5S$	-	-	-	-	-	-	-
$[Ni(ANBS)Cl_2]$	-	-	-	-	-	-	-
$[Cu(ANBS)(H_2O)_2Cl_2]$	-	35	24	-	-	-	-
$[Cu(ANBS)(H_2O)_2(ma)]$	-	-	-	-	-	-	-
$[Ni(ANBS)(pyph)]$	-	20	-	-	-	-	-

4. Conclusion

Depending on the information obtained, it showed the prepared new ligand as reagent were double-linked with the metals used via the azo group and (NH_2) substituted group, which gave very stable complexes. The octahedral shape was proposed for copper(II) complexes, while the square planar shape was proposed for nickel(II) complexes. The results showed the use of the prepared ligand as a good reagent to estimate nickel(II) and

copper(II), which provided highly sensitive, simple, fast and inexpensive methods. Some of the prepared compounds showed inhibitory activity on some types of bacteria *Serratia marcescens* and *Staphylococcus aureus*. It is possible to study their effect on cancer cells due to the ability of the complexes to mutate DNA and thus cause catabolic cell death. It is also possible to study the drug synergistic effect, which may increase the drug effectiveness against bacteria.

References

- [1] S. Masoud, S. Hemdan and M. Elsamra. Synthesis, ligating properties, thermal behavior, computational and biological studies of some azo-transition metal complexes. *Journal of Inorganic and Organometallic Polymers and Materials*, 33(2023), 120-137. <https://doi.org/10.1007/s10904-022-02483-x>
- [2] N. Verma, M. Rachamalla, S. Kumar, and K. Dua,. Assessment and impact of metal toxicity on wildlife and human health. In *Metals in water* (2023) (pp. 93-110). Elsevier. <https://doi.org/10.1016/B978-0-323-95919-3.00002-1>
- [3] K. Kyhoiesh and J. Al-Adilee. "Pt (IV) and Au (III) complexes with tridentate-benzothiazole based ligand: Synthesis, characterization, biological applications (antibacterial, antifungal, antioxidant, anticancer and molecular docking) and DFT calculation." *Inorganica Chimica Acta* 555 (2023): 121598.
- [4] A. Czyłkowska, M. Pitucha, S. Lanka, A. Raducka, B. Rogalewicz, M. Szczesio and P. Szymański,. Triazole-based Mn (II), Fe (II), Ni (II), Cu (II) and Zn (II) complexes as potential anticancer agents–Physicochemical properties, in silico predictions and in vitro activity. *Polyhedron*, (2024) 117106.. <https://doi.org/10.1016/j.poly.2024.117106>
- [5] M. El-Zahed, A. Diab, Z. El-Sonbati, G. Nozha, R. Issa, A. El-Mogazy, and M. Morgan,. Antibacterial, antifungal, DNA interactions, and antioxidant evaluation of Cu (II) Co (II), Ni (II), Mn (II) and UO₂ (II) mixed ligand metal complexes: Synthesis, characterization and molecular docking studies. *Materials Science and Engineering: B*, (2024) 299, 116998.. <https://doi.org/10.1016/j.mseb.2023.116998>
- [6] J. Babu, S. Daravath, M. Swathi and D. Ayodhya. Synthesis, anticancer, antibacterial, antifungal, DNA interactions, ADMET, molecular docking, and antioxidant evaluation of novel Schiff base and their Co (II), Ni (II) and Cu (II) complexes. *Results in Chemistry*, 6(2023), 101121.. <https://doi.org/10.1016/j.rechem.2023.101121>
- [7] K. Kyhoiesh and J. Al-Adilee, K.. Synthesis, spectral characterization, antimicrobial evaluation studies and cytotoxic activity of some transition metal complexes with tridentate (N, N, O) donor azo dye ligand. *Results in Chemistry*, 3(2021), 100245. <https://doi.org/10.1016/j.rechem.2021.100245>
- [8] A. Salamou, T. Jean-de-Dieu, F. Emmanuel, T. Germaine, T. Gabin, F. Simon and K. Jules-Roger. Synthesis, characterization, and antibacterial activity of a new poly azo compound containing N-arylsuccinimid and dibenzobarrelene moieties. *Heterocyclic Communications*, 29(2023), 20220157.. <https://doi.org/10.1515/hc-2022-0157>
- [9] K. Kyhoiesh and M. Hassan. "Synthesis, Characterization, in silico DFT, Molecular docking, ADMET Profiling Studies and Toxicity Predictions of Ag (I) Complex Derived from 4-Aminoacetophenone." *ChemistrySelect* 9.4 (2024): e202304429.
- [10] A. Gičević, L. Hindija and A. Karačić. Toxicity of azo dyes in pharmaceutical industry. In *CMBEBIH 2019: Proceedings of the International Conference on Medical and Biological Engineering, 16–18 May 2019, Banja Luka, Bosnia and Herzegovina* (2020) (pp. 581-587). Springer International Publishing.. https://doi.org/10.1007/978-3-030-17971-7_88
- [11] S. Belowar. Synthesis and biological study of newly synthesized AZO appended thiadiazolin heterocycles(2022).. <https://doi.org/10.24996/ijcs.2019.60.11.4>
- [12] S. Patai. The chemistry of diazonium and diazo groups (1978). (No Title).
- [13] S. Benkhaya, S. Mrabet and A. El Harfi. Classifications, properties, recent synthesis and applications of azo dyes. *Heliyon*, 6(2020) <https://doi.org/10.1016/j.heliyon.2020.e03271>
- [14] W. Weaver. Electrophilic aromatic substitution. *Organic Reaction Mechanisms 2019: An annual survey covering the literature dated January to December 2019*, (2023) 213-255.. <https://doi.org/10.1002/9781119608288.ch5b>
- [15] A. Yanagisawa, T. Heima, K. Watanabe and S. Haeno. Selective Propargylation of Diaryl Azo Compounds Using Metallic Barium. *Synlett*, 31(2020), 1817-1822. DOI: 10.1055/s-0040-1706414
- [16] T. Zhang, Z. Xie, L. Jiang, W. Zhao, S. Cao, B. Wang and Z. Zhao. Selective transfer hydrogenation coupling of nitroaromatics to azoxy/azo compounds by electron-enriched single Ni-N₄ sites on mesoporous N-doped carbon. *Chemical Engineering Journal*, (2022) 443, 136416.. <https://doi.org/10.1016/j.cej.2022.136416>
- [17] B. Singh, D. Mandelli and P. Pescarmona. Efficient and selective oxidation of aromatic amines to azoxy derivatives over aluminium and gallium oxide catalysts with nanorod morphology. *ChemCatChem*, 12(2020), 593-601.. <https://doi.org/10.1002/cctc.201901378>
- [18] B. Jiang, Y. Du and Z. Han. Palladium-mediated base-free and solvent-free synthesis of aromatic azo compounds from anilines catalyzed by copper acetate. *Green Processing and Synthesis*, 11(2022), 823-829.. <https://doi.org/10.1515/gps-2022-0070>
- [19] B. Mondal and S. Mukherjee. Cage encapsulated gold nanoparticles as heterogeneous photocatalyst for facile and selective reduction of nitroarenes to azo compounds. *Journal of the American Chemical Society*, 140(2018),

- 12592-12601..
<https://pubs.acs.org/doi/abs/10.1021/jacs.8b07767>
- [20] Z. Yan, X. Xie, Q. Song, F. Ma, X. Sui, Z. Huo and M. Ma. Tandem selective reduction of nitroarenes catalyzed by palladium nanoclusters. *Green Chemistry*, 22(2020), 1301-1307.. <https://doi.org/10.1039/C9GC03957K>
- [21] G. Wyasu and B. Myek. Synthesis of an azo dye and its cobalt complex derived from 3-aminophenol. *Communication in Physical Sciences*, 6(2020). <https://journalcps.com/index.php/volumes/article/view/148>
- [22] N. Tawfeeq, R. Majeed and A. Awad. Synthesis and spectroscopic study of gold Au (III) complexes from mixed ligands. *Synthesis*, 23(2019), 143-160.. <http://onljvetres.com/ligandabs2019.htm>
- [23] D. Perrin. *Buffers for pH and metal ion control*. Springer Science & Business Media(2012).
- [24] R. Cruickshank. *Medical microbiology: the practice of medical microbiology*, (1975) vol2..
- [25] D. Nandiyanto, R. Ragadhita and M. Fiandini. Interpretation of Fourier transform infrared spectra (FTIR): A practical approach in the polymer/plastic thermal decomposition. *Indonesian Journal of Science and Technology*, 8(2023), 113-126.. <https://doi.org/10.17509/ijost.v8i1.53297>
- [26] A. Naseem, T. Aziz, K. Ahmad, S. Parveen and M. Ashfaq. Rational synthesis and characterization of medicinal phenyl diazenyl-3-hydroxy-1h-inden-1-one azo derivatives and their metal complexes. *Journal of molecular structure*, 1227(2021), 129574.. <https://doi.org/10.1016/j.molstruc.2020.129574>
- [27] N. Tawfeeq, A. Awad and R. Majeed. SYNTHESIS, SPECTROSCOPIC STUDY AND BIOLOGICAL ACTIVITY FOR PD (II) COMPLEXES FROM MIXED LIGANDS. *BIOCHEMICAL AND CELLULAR ARCHIVES*, 19(2019) (Suppl 1), 2289-2295. http://www.connectjournals.com/file_full_text/3010500H_2289-2295.pdf
- [28] H. Obaid, S. Sultan and S. Al-Hamdani.. Synthesis, characterization and biological efficacies from some new dinuclear metal complexes for base 3-(3, 4-dihydroxyphenyl)-2-[(2-hydroxy-3-methylperoxy-benzylidene)-amino]-2-methyl propionic acid. *Indonesian journal of chemistry*, 20(2020), 1311-1322. <https://doi.org/10.22146/ijc.49842>
- [29] H. Ahmed and A. Mohammed. Metal (II) complexes derived from proline dithiocarbamate and ligand adducts phenathroline: Synthesis, characterization, biological activity and SEM study. In *AIP Conference Proceedings* (2024, May) (Vol. 3097, No. 1). AIP Publishing.. <http://dx.doi.org/10.13005/ojc/340340>
- [30] N. Alalam and S. Bashir. Analytical Applications of some N, NBPAD Schiff's base for Spectrophotometric Determination of Chromium (VI). *Chemistry Research Journal*, 9(2024), 86-93.. <https://doi.org/10.5281/zenodo.11275451>
- [31] N. Das and S. Agrawal. SENSITIVE AND HIGHLY SELECTIVE SPECTROPHOTOMETRY METHOD FOR DETERMINATION OF NICKEL. *NeuroQuantology*, 20(2022), 4305..
- [32] G. Rasulov, Z. Zalov, A. Mammadova and A. Huseynova. Spectroscopic studies of complexation cu, co, ni using aminophenols. determination of Cu (II), Co (II) and Ni (II) in wastewater, bottom sediments, oil and oil products Baku. *Processes of Petrochemistry and oil Refining*, 23(2022), 163-174. <https://www.ppor.az/jpdf/1-Rasulov-2-2022.pdf>
- [33] M. Elsharif, Y. Alzalouk, A. Zubi and S. Al-Ddarwish. Facile spectrophotometric determination of Cd (II) and Pb (II) using murexide reagent in mixed solvent system. *Chemistry International*, 8(2022), 148-156.. <https://doi.org/10.22034/pcbr.2022.338475.1222>
- [34] M. Ismail, M. Abou El Maaty, J. Jean-Claude and I. Mostafa. Synthesis, characterization and anticancer activity of new Zn (II) and MoO₂+ complexes of 2-amino-4, 6-mercaptotriazine. *Inorganic Chemistry Communications*, 106, (2019) 217-223... <https://doi.org/10.1016/j.inoche.2019.04.024>
- [35] D. Baghel and K. Banjare. Host-guest complexation between β-cyclodextrin and phosphonium-based ionic liquid and influence of its inclusion complex on the binding property of paracetamol drug. *Journal of Molecular Liquids*, 389, (2023) 122867 . <https://doi.org/10.1016/j.molliq.2023.122867>
- [36] H. Yoe and L. Jones. Colorimetric determination of iron with disodium-1, 2-dihydroxybenzene-3, 5-disulfonate. *Industrial & Engineering Chemistry Analytical Edition*, 16(1944), 111-115... <https://doi.org/10.1021/i560126a015>
- [37] A. Benosmane, , B. Gündüz, , A. Benaouida, C. Boukentoucha and H. Merzig.. Experimental structural and optoelectronic properties and theoretical investigation of novel square planar nickel (II) complex with (o-tolyldiazenyl) naphthalen-2-ol ligand. *Journal of Molecular Structure*, 1273,(2023)134254.. <https://doi.org/10.1016/j.molstruc.2022.134254>
- [38] K. Adhami, , H. Asadollahzadeh, M. Ghazizadeh.. Preconcentration and determination of nickel (II) and copper (II) ions, in vegetable oils by [TBP][PO₄] IL-based dispersive liquid-liquid microextraction technique, and flame atomic absorption spectrophotometry. *Journal of Food Composition and Analysis*, 89(2020), 103457.. <https://doi.org/10.1016/j.jfca.2020.103457>
- [39] H. Abo-Shama, H. El-Gendy, , S. Mousa, A. Hamouda, E. Yousuf, F. Hetta and E. Abdeen. Synergistic and antagonistic effects of metal nanoparticles in combination with antibiotics against some reference strains of pathogenic microorganisms. *Infection and drug resistance*, (2020)351-362. <https://doi.org/10.2147%2FIDR.S234425>
- [40] A. El-Bindary and M. Fathy. Azo naringenin-based copper (II) complex as DNA binder: Synthesis, spectroscopic characterization, and diverse biological potentials. *Applied Organometallic Chemistry*, 38(2024),e7460.. <https://doi.org/10.1002/aoc.7460>

- [41] M. Montilla-Suárez, L. dos Santos, B. de Araújo, H. Rodrigues, C. Tenorio, B. Soares and S. Correa. Structural elucidation of a new binuclear copper (II)/phenanthroline/2-(2, 4-dihydroxybenzoyl) benzoate complex by synchrotron radiation, DNA interaction and cytotoxicity against tumor cells. *Inorganic Chemistry Communications*, (2024) 112670.. <https://doi.org/10.1016/j.inoche.2024.112670>
- [42] A. Salih, T. Hassan, R. Majeed, J. Ibraheem, M. Hassan and S. Obaid. In vitro scolical activity of synthesised silver nanoparticles from aqueous plant extract against *Echinococcus granulosus*. *Biotechnology Reports*, 28(2020), e00545.. <https://doi.org/10.1016/j.btre.2020.e00545>
- [43] Y. Abdul-Jabbar, M. Hassan and J. Ibraheem. SYNERGISTIC EFFECT OF NICKEL COMPOSITE WITH THE ANTIBIOTICS GENTAMICIN, AMOXICILLIN AND FUSIDIC ACID AGAINST BACTERIAL PATHOGENS. *Biochemical & Cellular Archives*, 21(2021). <https://connectjournals.com/03896.2021.21.4685>
- [44] E. Lamey, O. Selim, M. Atia and E. Mowafy. Genes contributed on biofilm forming bacteria incriminated in various disease conditions in cattle. *Journal of Advanced Veterinary Research*, 13(2023),312-321.. <https://advetresearch.com/index.php/AVR/article/view/1221>